

PAPER • OPEN ACCESS

Infernal and exceptional edge modes: non-Hermitian topology beyond the skin effect

To cite this article: M Michael Denner *et al* 2023 *J. Phys. Mater.* **6** 045006

View the [article online](#) for updates and enhancements.

You may also like

- [Pressure driven long wavelength MHD instabilities in an axisymmetric toroidal resistive plasma](#)
J P Graves, M Coste-Sarguet and C Wahlberg
- [Non-Hermitian topological phases: principles and prospects](#)
Ayan Banerjee, Ronika Sarkar, Soumi Dey et al.
- [Neoclassical tearing mode seeding by coupling with infernal modes in low-shear tokamaks](#)
A. Kleiner, J.P. Graves, D. Brunetti et al.



PAPER

OPEN ACCESS

RECEIVED
3 May 2023REVISED
14 August 2023ACCEPTED FOR PUBLICATION
22 August 2023PUBLISHED
31 August 2023

Original Content from
this work may be used
under the terms of the
[Creative Commons
Attribution 4.0 licence](#).

Any further distribution
of this work must
maintain attribution to
the author(s) and the title
of the work, journal
citation and DOI.



Infernal and exceptional edge modes: non-Hermitian topology beyond the skin effect

M Michael Denner¹ , Titus Neupert¹ and Frank Schindler^{2,*} ¹ Department of Physics, University of Zürich, Winterthurerstrasse 190, 8057 Zürich, Switzerland² Blackett Laboratory, Imperial College London, London SW7 2AZ, United Kingdom

* Author to whom any correspondence should be addressed.

E-mail: f.schindler@imperial.ac.uk**Keywords:** band topology, non-Hermitian, edge statesSupplementary material for this article is available [online](#)

Abstract

The classification of point gap topology in all local non-Hermitian (NH) symmetry classes has been recently established. However, many entries in the resulting periodic table have only been discussed in a formal setting and still lack a physical interpretation in terms of their bulk-boundary correspondence. Here, we derive the edge signatures of all two-dimensional phases with intrinsic point gap topology. While in one dimension point gap topology invariably leads to the NH skin effect, NH boundary physics is significantly richer in two dimensions. We find two broad classes of non-Hermitian edge states: (1) *infernal points*, where a skin effect occurs only at a single edge momentum, while all other edge momenta are devoid of edge states. Under semi-infinite boundary conditions, the point gap thereby closes completely, but only at a single edge momentum. (2) NH exceptional point *dispersions*, where edge states persist at all edge momenta and furnish an anomalous number of symmetry-protected exceptional points. Surprisingly, the latter class of systems allows for a finite, non-extensive number of edge states with a well defined dispersion along all generic edge terminations. Concomitantly, the point gap only closes along the real and imaginary eigenvalue axes, realizing a novel form of NH spectral flow.

1. Introduction

The study of non-Hermitian (NH) band theory has gained increasing attention in recent years, with potential applications in optics [1–6], condensed matter physics [7–29], and quantum information processing [30–35]. NH topological phases have attracted particular interest due to their unconventional bulk-boundary correspondence [36–59]. One of the prime examples is the NH skin effect, in which an extensive number of states localizes at the boundary of a one-dimensional (1D) system [60–69]. The NH skin effect can be enhanced by symmetries, for example to a \mathbb{Z}_2 skin effect in 1D time reversal-symmetric systems [66]. However, NH topological phases are not limited to 1D: NH internal symmetries give rise to a total of 38 symmetry classes, which were topologically classified for all spatial dimensions in the seminal works of references [40, 66, 70]. The physical consequence of this classification are new forms of dynamical and topologically protected edge states. Intrinsically NH systems have a point-gapped bulk spectrum, in which complex eigenvalues surround a region devoid of eigenstates [40, 50]. Crucially, such Hamiltonians cannot be adiabatically deformed to purely (anti-) Hermitian limits. While the NH skin effect constitutes the bulk-boundary correspondence of nontrivial 1D point gap topology, to date, there is no systematic study of the boundary physics of two-dimensional (2D) NH systems.

In this paper, we derive the edge signature of all intrinsically point-gapped phases in 2D. These phases cannot be trivialized by coupling to NH line-gapped phases or symmetry-preserving perturbations as long as the point gap remains open [66]. To establish the bulk-boundary correspondence, we focus on the spectrum with semi-infinite boundary conditions (SIBC). The SIBC spectrum is related to the ϵ -pseudospectrum, which captures the behavior of a Hamiltonian under small perturbations of order $\mathcal{O}(\epsilon)$ [66, 69]. As such, it

provides a robust observable for NH systems, which in general can be highly sensitive to infinitesimal errors. Moreover, only the SIBC spectrum—and not the spectrum under open boundary conditions (OBC) – allows for a one-to-one correspondence between the bulk topological invariants, calculated in periodic boundary conditions (PBC), and boundary dispersion [71]. Our approach, therefore, differs from the OBC treatment of Nakamura *et al* [72]. Depending on the NH symmetry class, the boundary response falls into one of two classes:

- (1) **Infernal points (IPs):** The point gap remains open at generic values of the edge momentum k_{\parallel} , but completely fills up with an extensive number of SIBC edge states at one of $k_{\parallel} = 0, \pi$ (see figure 1(a)).
- (2) **Exceptional points (EPs):** As k_{\parallel} is varied, the edge state disperses with a square-root singularity for real and imaginary parts of the spectrum [73–75]. Concomitantly, the SIBC point gap only fills up along the real and imaginary axes (see figure 2(a)).

Both types of edge states are topologically protected and anomalous in the sense that they cannot be realized in a 1D lattice system. We begin by discussing case (1) for the specific example of NH symmetry class AII^{\dagger} , highlighting the unique spectral signature and edge state. Next, we derive the general criterion for infernal edge modes. As an example for a NH symmetry class without an IP, we then discuss case (2) in NH symmetry class $\text{AIII}^{\text{S-}}$. Based on these two paradigmatic signatures, we identify the nature of edge state for each NH symmetry class that allows for intrinsic point gap topology in table 1.

2. Infernal edge modes

We begin our survey of edge modes with the specific example of NH symmetry class AII^{\dagger} , which was also discussed in the appendix of Okuma *et al* [66]. This class is characterized by a pseudo-time-reversal symmetry $U_{\mathcal{T}}\mathcal{H}(\mathbf{k})^T U_{\mathcal{T}}^{\dagger} = \mathcal{H}(-\mathbf{k})$, where $U_{\mathcal{T}}$ is a unitary operator obeying $U_{\mathcal{T}}U_{\mathcal{T}}^* = -1$. The intrinsic point gap topology is classified by a \mathbb{Z}_2 invariant $\nu(E_0) \in \{0, 1\}$ [40], where E_0 is any eigenvalue inside the point gap. Relying on the topological equivalence between a NH Hamiltonian H and an extended Hermitian Hamiltonian (EHH) \bar{H} , defined as [76, 77]

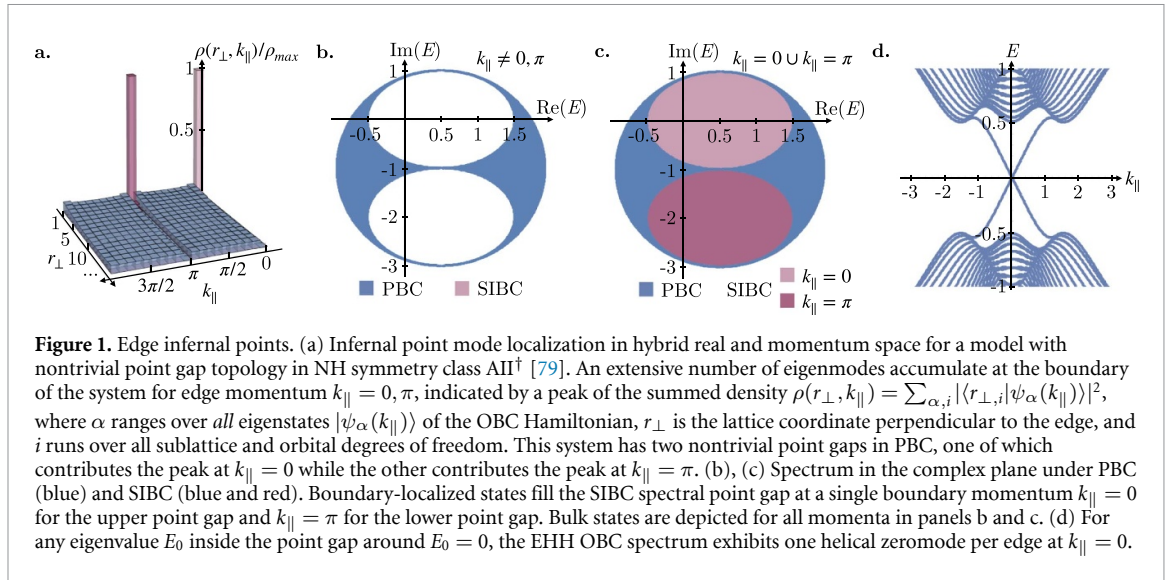
$$\bar{H} = \begin{pmatrix} 0 & H - E_0 \\ H^{\dagger} - E_0^* & 0 \end{pmatrix}, \quad (1)$$

we can derive the signature of the nontrivial point gap phase with $\nu = 1$. The presence of a point gap of H around $E = E_0$ results in a gapped spectrum of \bar{H} around zero energy. (We only refer to the eigenvalues of \bar{H} as energies because the eigenvalues of the NH Hamiltonian H involve not only energies but also lifetimes.) On the other hand, the existence of exact topological zero-energy eigenvalues in \bar{H} corresponds to protected states at $E = E_0$ within the NH point gap. The EHH for NH class AII^{\dagger} is in Hermitian symmetry class DIII, regardless of the choice of E_0 . Class DIII Hermitian systems are also \mathbb{Z}_2 -classified in 2D [78], so that a nontrivial point gap in NH class AII^{\dagger} maps to a topological superconductor phase in class DIII. This phase hosts helical boundary modes that cross zero energy at a time-reversal invariant momentum (TRIM) (see figure 1(d)). Crucially, due to the time-reversal (TRS), particle-hole (PHS) and chiral symmetry (CS) of Hermitian class DIII, the Kramers pair cannot be moved away from the TRIM and zero energy. In the NH SIBC spectrum, this zeromode corresponds to a single edge-localized state at complex eigenvalue E_0 in the point gap (see figure 1(c)) [66]. By repeating this construction for all E_0 within the point gap, we obtain a number of modes localized at the boundary that scales with the linear system size. However, since the helical crossing of the EHH edge mode cannot move away from the TRIM even as E_0 is varied, this extensive accumulation of modes appears only for a single edge momentum $k_{\parallel} \in \{0, \pi\}$ (see figure 1(a)). For *all* other momenta, the point gap remains empty (see figure 1(b)). This dispersion with k_{\parallel} constitutes an intrinsically NH edge state that we dub *IP* in reminiscence of the infinitely steep surface dispersion observed in some 3D NH point-gapped systems [53]. (See the supplemental material [79] for a discussion of the OBC and ϵ -pseudospectrum associated with an IP.)

The derivation outlined above is completely general and does not rely on a particular model Hamiltonian, but only the respective symmetry class as well as the presence of a topologically nontrivial point gap. In order to further rationalize the IP, we now consider a representative Hamiltonian for class AII^{\dagger} and solve for the edge state within a Dirac approximation. The full Hamiltonian is given in the supplemental material [79], for our purposes it is enough to consider its expansion to first order around $\mathbf{k} = 0$:

$$\mathcal{H}(\mathbf{k}) = [im + \Delta] \sigma_0 + k_x \sigma_x - k_y \sigma_z. \quad (2)$$

Here, m and Δ are real parameters, σ_{μ} are the Pauli matrices ($\mu = 0, x, y, z$), and $U_{\mathcal{T}} = i\sigma_y$.



We want to stress that the full bulk Hamiltonian of this model [79] includes non-trivial non-Hermitian momentum dependent terms not present in its Dirac expansion. Therefore, this Hamiltonian does not simply result from an imaginary shift of a Hermitian model. In fact, a simple imaginary shift of a Hermitian topological insulator always results in a line-gapped NH model. Here we focus on intrinsically point-gapped NH systems to exclude such a scenario.

To obtain the edge states of $\mathcal{H}(\mathbf{k})$, we consider OBC in x -direction, and model the transition to the surrounding vacuum by a domain wall in m , whose sign governs the bulk NH topology [66, 80]. Consequently we solve

$$\{[im(x) + \Delta]\sigma_0 - i\partial_x\sigma_x - k_y\sigma_z\} \psi(x) = E\psi(x), \quad (3)$$

with $E \in \mathbb{C}$, for the right eigenfunction $\psi(x)$. Here, the mass $m(x) = m_0 \text{sgn}(x)$, $m_0 > 0$, changes sign at $x = 0$. Defining

$$\omega_{\pm}^2 = \underbrace{[m_0 + i(k_y + E - \Delta)]}_{\alpha_{+}} \underbrace{[m_0 - i(k_y - E + \Delta)]}_{\alpha_{-}}, \quad (4)$$

the normalizable solution in the right half plane (+) reads

$$\psi_{+}(x) = \frac{1}{\mathcal{N}} e^{-\omega_{+}x} \begin{bmatrix} \omega_{+} \\ \alpha_{+} \\ -1 \end{bmatrix}^T, \quad (5)$$

where \mathcal{N} is a normalization constant. Similarly, defining

$$\omega_{-}^2 = \underbrace{[m_0 + i(k_y - E + \Delta)]}_{\beta_{+}} \underbrace{[m_0 - i(k_y + E - \Delta)]}_{\beta_{-}}, \quad (6)$$

the normalizable solution in the left halfspace (−) reads

$$\psi_{-}(x) = \frac{1}{\mathcal{N}} e^{\omega_{-}x} \begin{bmatrix} \omega_{-} \\ \beta_{-} \\ -1 \end{bmatrix}^T. \quad (7)$$

Matching the solutions across the domain wall yields

$$\psi_{+}(0) = \psi_{-}(0) \Leftrightarrow \frac{\alpha_{-}}{\alpha_{+}} = \frac{\beta_{+}}{\beta_{-}}. \quad (8)$$

We now have to distinguish three cases: first, when neither β_{-} nor α_{+} are equal to zero, the matching constraint implies $k_y = 0$. However, all possible (real and imaginary) energies E are allowed. Furthermore, the case $\beta_{-} = 0$ is not admissible because the solution should decay in the vacuum. In the bulk however, this case might be tolerated, so we can consider $\alpha_{+} = 0$. From equation (8), finite $\beta_{\pm} \neq 0$ additionally implies $\alpha_{-} = 0$, again resulting in $k_y = 0$. Consequently, away from $k_y = 0$ no edge state solution exists. At $k_y = 0$, however, we obtain infinitely many boundary modes, with arbitrary $E \in \mathbb{C}$. Concomitantly, the entire NH point gap fills with edge-localized states at a single momentum, the defining characteristic of an IP. This

Table 1. NH bulk-boundary correspondence in 2D. We list all NH symmetry classes with intrinsic point gap topology [40]. The symmetry class labels refer to a given NH Altland–Zirnbauer (AZ) class or its AZ^\dagger counterpart, in some cases supplemented by an additional sublattice symmetry (SLS) S , which for NH systems is different from the AZ chiral symmetry (CS) [40]. The subscript of SLS determines whether SLS commutes (+) or anticommutes (−) with the respective AZ symmetry. If both time-reversal symmetry (TRS) and particle-hole symmetry (PHS) are present, the first subscript refers to TRS and the second one to PHS. The symmetry classes are identified by the square of TRS, acting as $U_{\mathcal{T}}\mathcal{H}(\mathbf{k})^*U_{\mathcal{T}}^\dagger = \mathcal{H}(-\mathbf{k})$, and PHS, defined by $U_{\mathcal{P}}\mathcal{H}(\mathbf{k})^T U_{\mathcal{P}}^\dagger = -\mathcal{H}(-\mathbf{k})$, or TRS^\dagger , denoted by $U_{\mathcal{T}}\mathcal{H}(\mathbf{k})^T U_{\mathcal{T}}^\dagger = \mathcal{H}(-\mathbf{k})$, and PHS^\dagger , expressed as $U_{\mathcal{P}}\mathcal{H}(\mathbf{k})^* U_{\mathcal{P}}^\dagger = -\mathcal{H}(-\mathbf{k})$ (second column). Their intrinsic point gap classification (third column) is reproduced from Okuma *et al* [66]. The edge states are identified as either an infernal point (IP) or an anomalous number of exceptional points (EP) per edge and point gap. Their multiplicity is denoted in parentheses.

Class	Symmetry			Classification		Edge mode
	TRS ^(†)	PHS ^(†)	CS	2D	1D	
AII [†]	−1	—	—	\mathbb{Z}_2	\mathbb{Z}_2	IP (1x)
DIII [†]	−1	+1	1	\mathbb{Z}_2	\mathbb{Z}_2	IP (1x)
BDI ^{S+-}	+1	+1	1	\mathbb{Z}_2	\mathbb{Z}_2	IP (1x)
D ^{S-}	—	+1	—	\mathbb{Z}_2	\mathbb{Z}_2	IP (1x)
AIII ^{S-}	—	—	1	\mathbb{Z}_2	0	EP (1x)
DIII ^{S+-}	−1	+1	1	\mathbb{Z}_2	0	EP (2x)
CII ^{S-+}	−1	−1	1	\mathbb{Z}_2	0	EP (2x)
CII ^{S+-}	−1	−1	1	\mathbb{Z}_2	0	EP (2x)
CI ^{S-+}	+1	−1	1	\mathbb{Z}_2	0	EP (2x)

result holds irrespective of the specific model Hamiltonian used above as long as the point gap is not closed and the symmetries of class AII[†] are preserved: see the supplemental material [79] for an explicit study on the persistence of the IP under generic symmetry-allowed perturbations to equation (2) respecting the point gap topology, i.e. they do not close or close and reopen the point gap, including traceless Pauli matrices with imaginary and k -dependent prefactors. We can also calculate the left eigenstates of $\mathcal{H}(\mathbf{k})$ in equation (2), which are the right eigenstates of $\mathcal{H}(\mathbf{k})^\dagger$. The overlap between left and right eigenstates vanishes, similar to the NH skin effect in 1D [66].

Notably, an IP cannot be realized in a 1D lattice system with a finite-dimensional unit cell Hilbert space. Instead, such an edge mode realizes an anomalous dispersion whose discontinuity and TRIM skin effect capitalizes on a topologically nontrivial 2D bulk. To generalize beyond the specific example given above, we investigate the presence of infernal edge modes in all NH symmetry classes with intrinsic point gap topology. We find that a point gap-nontrivial 2D system in a given NH symmetry class exhibits an IP *if and only if* this symmetry class also has a nontrivial 1D point gap classification [79]. The NH symmetry classes satisfying this criterion are summarized in table 1.

3. Exceptional edge modes

We next consider the example of NH symmetry class AIII^{S-}, which contains a CS $U_C\mathcal{H}(\mathbf{k})U_C^\dagger = -\mathcal{H}(\mathbf{k})^\dagger$ as well as a sublattice symmetry $\mathcal{S}\mathcal{H}(\mathbf{k})\mathcal{S}^\dagger = -\mathcal{H}(\mathbf{k})$ with $\{U_C, \mathcal{S}\} = 0$ [40]. This symmetry class quantizes the 2D point gap topological invariant $C_1 \in \mathbb{Z}$ [40]. However, the classification of intrinsic point gap topology in AIII^{S-} is only \mathbb{Z}_2 , corresponding to $C_1 \pmod{2}$: all phases with even C_1 can be trivialized by coupling to line-gapped phases [66]. To derive the topological edge state of the phase where $|C_1| = 1$, we again rely on the EHH for a given eigenvalue E_0 inside the point gap (equation (1)). Importantly, and unlike for symmetry classes protecting infernal edge modes, the EHH enjoys distinct Hermitian symmetries depending on the choice of E_0 [79]. For purely real ($E_0 \in \mathbb{R}$) or imaginary energies ($E_0 \in i\mathbb{R}$), the EHH can be block-diagonalized into two matrix blocks that are mapped to each other under CS (see below for details) [79]. Each block individually only satisfies Hermitian class A, which is \mathbb{Z} -classified in 2D [78]. The EHH associated with $|C_1| = 1$ then corresponds to an insulator with Chern number $C = \pm 1$ in each of the two blocks, giving rise to a total of one right and one left-moving chiral mode per edge. These modes are protected from gapping out due to the symmetries present for $E_0 \in \mathbb{R}$ ($E_0 \in i\mathbb{R}$), and cross zero energy at distinct edge momenta depending on the particular choice of E_0 (see figure 2(b), left). The corresponding NH SIBC spectrum therefore exhibits edge states dispersing as a function of the edge momentum. However, the edge states cross the point gap only along the real and imaginary axis (see figure 2(a)). Away from these axes, the SIBC spectrum shows no in-gap states, because the EHH symmetries reduce for generic $E_0 \in \mathbb{C}$ and do not anymore prevent hybridization between the two chiral edge modes [78, 79] (see figure 2(b), right). We note that even though the NH edge states only traverse the point gap along special axes, they cannot be moved away from these axes or out of the point gap due to the symmetry of NH class AIII^{S-}.

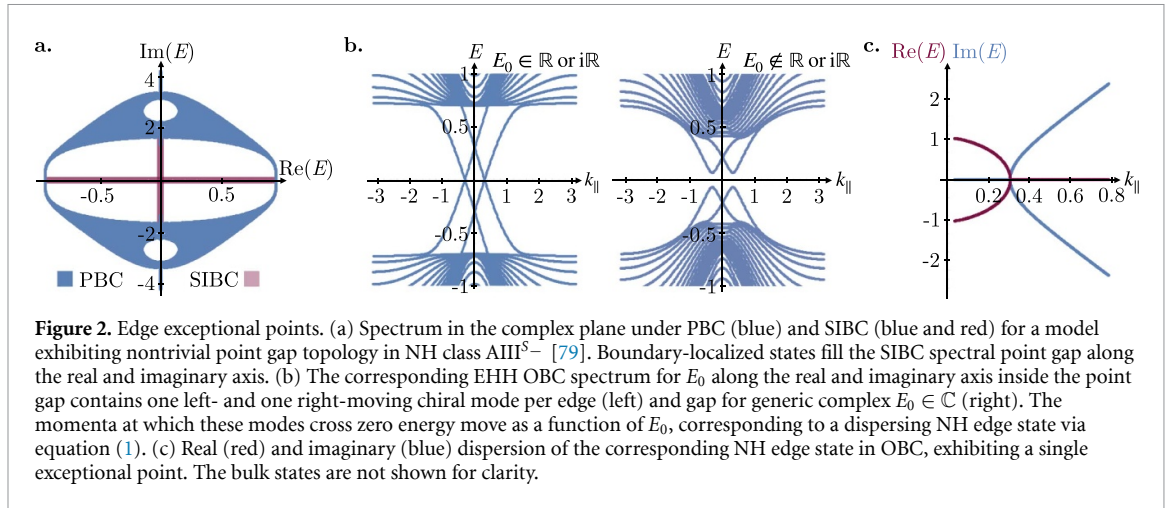


Figure 2. Edge exceptional points. (a) Spectrum in the complex plane under PBC (blue) and SIBC (blue and red) for a model exhibiting nontrivial point gap topology in NH class $AIII^{S-}$ [79]. Boundary-localized states fill the SIBC spectral point gap along the real and imaginary axis. (b) The corresponding EHH OBC spectrum for E_0 along the real and imaginary axis inside the point gap contains one left- and one right-moving chiral mode per edge (left) and gap for generic complex $E_0 \in \mathbb{C}$ (right). The momenta at which these modes cross zero energy move as a function of E_0 , corresponding to a dispersing NH edge state via equation (1). (c) Real (red) and imaginary (blue) dispersion of the corresponding NH edge state in OBC, exhibiting a single exceptional point. The bulk states are not shown for clarity.

We now show that the NH edge dispersion realizes a single EP (also evident from the numerical result of figure 2(c)). Due to the absence of a NH skin effect at all edge momenta, we can derive the edge state by writing down the effective edge EHH and then inverting equation (1) to obtain the effective edge NH Hamiltonian. At $E_0 = 0$, the EHH for NH class $AIII^{S-}$ features three *distinct* chiral symmetries, \bar{U}_C , $\bar{\Sigma}_C$, and \bar{S} that satisfy the algebra $\{\bar{U}_C, \bar{\Sigma}_C\} = 0$, $\{\bar{U}_C, \bar{S}\} = 0$, and $[\bar{\Sigma}_C, \bar{S}] = 0$ [79]. The minimal EHH matrix dimension that realizes this algebra is 4. Using the Pauli matrices τ_μ, σ_μ ($\mu = 0, x, y, z$), one possible representation is given by $\bar{U}_C = \tau_x \sigma_z$, $\bar{\Sigma}_C = \tau_z \sigma_0$, and $\bar{S} = \tau_0 \sigma_x$, which conforms with the basis choice in equation (1) where $\bar{\Sigma}_C$ is diagonal. We now combine the three chiral symmetries to form two commuting unitary symmetries $\bar{U}_1 = \bar{U}_C \bar{S}$ and $\bar{U}_2 = \bar{U}_C \bar{\Sigma}_C$ that both square to -1 . Correspondingly, at $E_0 = 0$, all eigenstates of the effective edge EHH $\bar{\mathcal{H}}_{\text{edge}}(k)$ are labelled by a pair of quantum numbers $(\pm i, \pm i)$ that denote the eigenvalues of \bar{U}_1 and \bar{U}_2 , respectively. Any of the three chiral symmetries anti-commute with both unitary symmetries, and therefore flip *both* their eigenvalues. In the common eigenbasis of \bar{U}_1 and \bar{U}_2 given by $\{|i, i\rangle, |-i, -i\rangle, |i, -i\rangle, |-i, i\rangle\}$, we therefore posit

$$\bar{\mathcal{H}}_{\text{edge}}(k) = \begin{pmatrix} \nu k \sigma_z & 0 \\ 0 & \Delta \sigma_z \end{pmatrix}, \quad (9)$$

where ν is the Fermi velocity of the chiral modes and $\Delta > 0$ is a constant energy. Without loss of generality, this Hamiltonian realizes a single pair of left- and right-moving chiral modes together with a pair of gapped bands at energies $\pm \Delta$ that are necessary to conform with the symmetry realization chosen above. To satisfy the chiral symmetries, the two chiral modes appear with opposite eigenvalues of \bar{U}_1 and \bar{U}_2 , preventing them from hybridization at all real $E_0 \in \mathbb{R}$ (where only \bar{U}_1 survives), and all imaginary $E_0 \in i\mathbb{R}$ (where only \bar{U}_2 survives), but not at generic $E_0 \in \mathbb{C}$. To obtain the corresponding NH Hamiltonian, we transform equation (9) back to the basis of equation (1) in which the common eigenvectors of \bar{U}_1 and \bar{U}_2 read $\psi_{(\lambda_1 i, \lambda_2 i)} = (1, \lambda_1 \lambda_2, -\lambda_2 i, \lambda_1 i)^T / 2$ for $\lambda_{1,2} = \pm 1$. The transformed matrix then assumes the canonical EHH form of equation (1), from which one can extract the effective NH edge Hamiltonian

$$\mathcal{H}_{\text{edge}}(k) = \frac{i}{2}(\nu k - \Delta) \sigma_z + \frac{1}{2}(\nu k + \Delta) \sigma_y. \quad (10)$$

The NH spectrum $E_{\text{edge}}(k) = \pm \sqrt{\nu k \Delta}$ indeed realizes a single EP as k is varied, analogous to the numerical result of figure 2(c).

We note that EPs generically occur in 2D rather than 1D, because two momenta must be tuned to ensure a two-fold degeneracy between NH bands absent symmetry [81]. However, imposing NH symmetry class $AIII^{S-}$ reduces the number of degeneracy constraints to one, thereby ensuring that also in the 1D case EPs can only be annihilated in pairs [73–75]. As a consequence, the presence of a single EP in figure 2(c) and equation (10) implies an anomaly: any odd number of EPs cannot be realized in a regularized lattice system due to the NH fermion doubling theorem [82].

We furthermore note that trivial and non-trivial unpaired EPs can also exist beyond the restrictions of the fermion doubling theorem as recently shown in [83]. The EPs discussed here are, however, stable to any symmetry-allowed perturbation that does not close the point gap as it is ramped up, and do not rely on a braiding of eigenvalues in 2D momentum space [83]. Instead, they appear on the 1D boundary of a 2D system and are a direct consequence of the anomalous edge states of the corresponding EHH. Hence, edge EPs cannot be realized in any purely 1D model and correspond to an anomaly also in the NH setting.

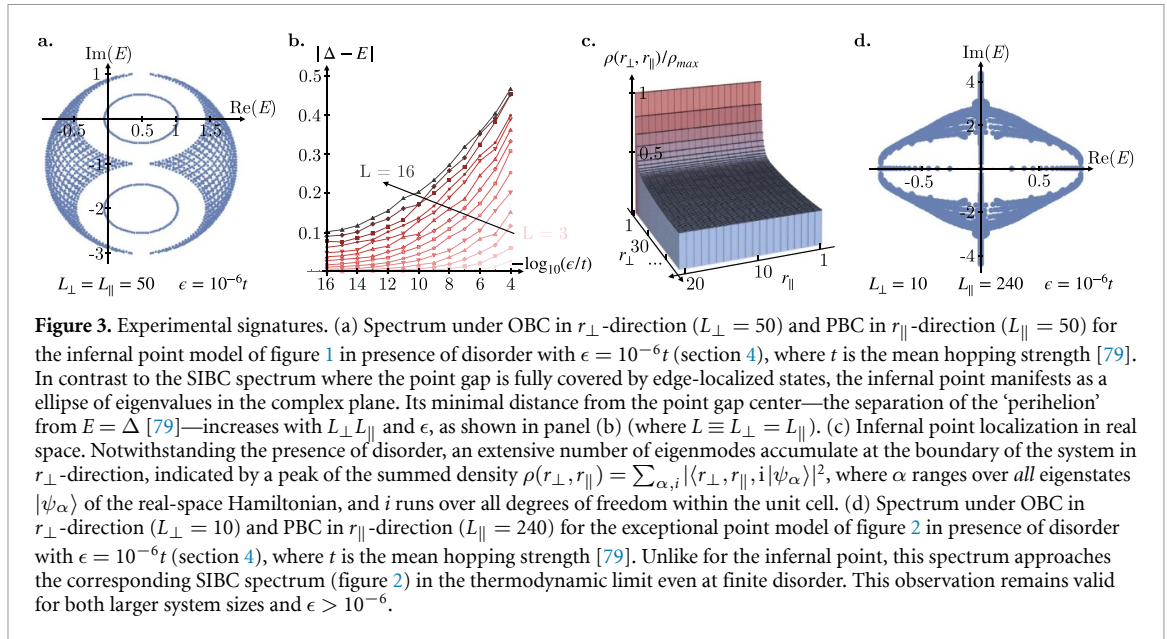


Figure 3. Experimental signatures. (a) Spectrum under OBC in r_{\perp} -direction ($L_{\perp} = 50$) and PBC in r_{\parallel} -direction ($L_{\parallel} = 50$) for the infernal point model of figure 1 in presence of disorder with $\epsilon = 10^{-6}t$ (section 4), where t is the mean hopping strength [79]. In contrast to the SIBC spectrum where the point gap is fully covered by edge-localized states, the infernal point manifests as an ellipse of eigenvalues in the complex plane. Its minimal distance from the point gap center—the separation of the ‘perihelion’ from $E = \Delta$ [79]—increases with $L_{\perp}L_{\parallel}$ and ϵ , as shown in panel (b) (where $L \equiv L_{\perp} = L_{\parallel}$). (c) Infernal point localization in real space. Notwithstanding the presence of disorder, an extensive number of eigenmodes accumulate at the boundary of the system in r_{\perp} -direction, indicated by a peak of the summed density $\rho(r_{\perp}, r_{\parallel}) = \sum_{\alpha, i} |\langle r_{\perp}, r_{\parallel}, i | \psi_{\alpha} \rangle|^2$, where α ranges over all eigenstates $|\psi_{\alpha}\rangle$ of the real-space Hamiltonian, and i runs over all degrees of freedom within the unit cell. (d) Spectrum under OBC in r_{\perp} -direction ($L_{\perp} = 10$) and PBC in r_{\parallel} -direction ($L_{\parallel} = 240$) for the exceptional point model of figure 2 in presence of disorder with $\epsilon = 10^{-6}t$ (section 4), where t is the mean hopping strength [79]. Unlike for the infernal point, this spectrum approaches the corresponding SIBC spectrum (figure 2) in the thermodynamic limit even at finite disorder. This observation remains valid for both larger system sizes and $\epsilon > 10^{-6}$.

We investigate all 2D NH symmetry classes with intrinsic point gap topology and find that exceptional edge modes arise whenever there is no IP, as summarized in table 1 (see the supplemental material [79] for details). Notably, certain NH symmetry classes show two EPs on their boundary. This edge response is, however, still anomalous because 1D lattice systems in these symmetry classes can only support a multiple of four EPs.

4. Experimental relevance

In our discussion of infernal and exceptional edge modes, we have so far focussed on the SIBC spectrum because it is equal to the ϵ -pseudospectrum of the corresponding OBC system [66, 69] for an ϵ that is exponentially small in the linear system size L (see also section 1). For clarity, we here only assume OBC in one direction and maintain PBC in the other, and consider full OBC later. We now study to what extent infernal and EPs are measurable at the boundaries of realistic experimental samples where L is thermodynamically large but ϵ remains finite. Notably, we focus on a single-particle picture. The extensive accumulation of states at an IP violates Pauli’s exclusion principle for fermionic many-body systems, and is hence modified in this context [84]. Bosonic or classical platforms will, however, still realize an essentially single-particle skin effect. At the same time, EPs survive even in a generic (bosonic and fermionic) many-body setting, similar to the boundary states of a Hermitian topological insulator.

We model the error ϵ by introducing uniformly distributed on-site disorder $V_{\epsilon} = \sum_{\mathbf{r}, i} \delta_{\mathbf{r}, i} |\mathbf{r}, i\rangle \langle \mathbf{r}, i|$ to the respective real-space Hamiltonian [85], with δ_i drawn uniformly from the range $[-\epsilon, +\epsilon]$. Here, \mathbf{r} ranges over all unit cells and i labels intra-unit cell degrees of freedom.

We find that infernal and exceptional edge modes differ drastically in their response to small finite disorder. For IP systems with OBC along one direction, the point gap remains empty as long as the linear system size L is sufficiently large and $\epsilon > 0$ is a finite L -independent constant (we assume a quadratic system of area L^2 for simplicity). This can be understood by noting that at any given L and ϵ , the OBC edge states form an ellipse in the complex plane (figure 3(a)) whose minimal radius increases with L and ϵ (figure 3(b)). We conclude that the spectral signature of edge IPs is highly sensitive to disorder in the thermodynamic limit and difficult to observe. However, the localization profile of eigenstates prevails even when they do not cover the point gap: an extensive number of eigenstates still accumulates at the OBC edges irrespective of the presence of disorder (figure 3(c)). In stark contrast, we find that edge EPs are unaffected by the presence of finite disorder: their OBC spectrum hosts edge states along real and imaginary axes in the complex plane (figure 3(d)) and approaches the SIBC spectrum in the thermodynamic limit. Similarly, their real space localization in OBC for one and two directions is not altered (see the supplemental material [79] for the analog of figure 3(c) for an edge EP).

For OBC in two directions, the IP edge loses also its skin effect in addition to its in-gap states [69]. On the other hand, the EP system remains largely unaffected in full OBC and still displays in-gap states along the real and imaginary axes [79].

5. Discussion

We have derived the edge modes of 2D NH phases with intrinsic point gap topology, providing a physical interpretation of the classification in references [40, 66, 70]. We find anomalous IP and EP edge modes that drastically differ in their real-space localization profile, dispersion with parallel edge momentum, and spectral stability to finite disorder. They both capitalize on a nontrivial NH bulk, in the sense that neither of them can be realized in a 1D NH lattice model. Several questions deserve further study: Can one set up a field theory for the IP anomaly, which seems to involve an effective edge Hamiltonian $\mathcal{H}_{\text{edge}}(k) \propto \delta(k)$? What is the fundamental physical difference between the types of point gap topology that induce skin effects, necessitating a SIBC treatment, and those that give rise to continuous NH dispersions, more similar in spirit to the Hermitian case and well-behaved in OBC? What are their dynamical consequences, e.g. in terms of wavepacket propagation? Are there NH edge modes that are qualitatively distinct from IPs and EPs in 3D systems or in presence of crystalline symmetries? Answering these questions is crucial for leveraging NH band topology in a realistic practical setting.

Data availability statement

All data that support the findings of this study are included within the article (and any supplementary files).

Acknowledgments

We thank Shinsei Ryu, Tomáš Bzdušek, Abhinav Prem and Kohei Kawabata for helpful discussions. We also thank the Kavli Institute for Theoretical Physics for hosting during completion of this work. M M D acknowledges support from a Forschungskredit of the University of Zurich (Grant No. FK-22-085) and thanks the Princeton Center for Theoretical Science for hosting during some stages of this work. This project has received funding from the European Research Council (ERC) under the European Union's Horizon 2020 research and innovation programme (ERC-StG-Neupert-757867-PARATOP). F S was supported by a fellowship at the Princeton Center for Theoretical Science. This research was supported in part by the National Science Foundation under Grant No. NSF PHY-1748958.

ORCID iDs

M Michael Denner  <https://orcid.org/0000-0002-1762-9687>

Titus Neupert  <https://orcid.org/0000-0003-0604-041X>

Frank Schindler  <https://orcid.org/0000-0001-8113-0998>

References

- [1] Feng L, El-Ganainy R and Ge Li 2017 Non-Hermitian photonics based on parity–time symmetry *Nat. Photon.* **11** 752–62
- [2] Midya B, Zhao H and Feng L 2018 Non-Hermitian photonics promises exceptional topology of light *Nat. Commun.* **9** 2674
- [3] Miri M-A and Alù A 2019 Exceptional points in optics and photonics *Science* **363** eaar7709
- [4] Gong Z, Bello M, Malz D and Kunst F K 2022 Bound states and photon emission in non-Hermitian nanophotonics *Phys. Rev. A* **106** 053517
- [5] Roccati F, Lorenzo S, Calajò G, Palma G M, Carollo A and Ciccarello F 2022 Exotic interactions mediated by a non-hermitian photonic bath *Optica* **9** 565–71
- [6] Roccati F, Bello M, Gong Z, Ueda M, Ciccarello F, Chenu A and Carollo A 2023 Hermitian and non-Hermitian topology from photon-mediated interactions (arXiv:2303.00762)
- [7] Kozii V and Fu L 2017 Non-Hermitian topological theory of finite-lifetime quasiparticles: prediction of bulk fermi arc due to exceptional point (arXiv:1708.05841)
- [8] Yoshida T, Peters R and Kawakami N 2018 Non-Hermitian perspective of the band structure in heavy-fermion systems *Phys. Rev. B* **98** 035141
- [9] Shen H and Fu L 2018 Quantum oscillation from in-gap states and a non-Hermitian Landau level problem *Phys. Rev. Lett.* **121** 026403
- [10] Carl Budich J C, Carlström J, Kunst F K and Bergholtz E J 2019 Symmetry-protected nodal phases in non-hermitian systems *Phys. Rev. B* **99** 041406
- [11] Herviou L, Regnault N and Bardarson J H 2019 Entanglement spectrum and symmetries in non-Hermitian fermionic non-interacting models *SciPost Phys.* **7** 069
- [12] Avila J, Peñaranda F, Prada E, San-Jose P and Aguado R 2019 Non-hermitian topology as a unifying framework for the Andreev versus Majorana states controversy *Commun. Phys.* **2** 133
- [13] Hamazaki R, Kawabata K and Ueda M 2019 Non-hermitian many-body localization *Phys. Rev. Lett.* **123** 090603
- [14] Michishita Y, Yoshida T and Peters R 2020 Relationship between exceptional points and the Kondo effect in *f*-electron materials *Phys. Rev. B* **101** 085122
- [15] Michishita Y and Peters R 2020 Equivalence of effective non-hermitian hamiltonians in the context of open quantum systems and strongly correlated electron systems *Phys. Rev. Lett.* **124** 196401

- [16] Nagai Y, Qi Y, Isobe H, Kozii V and Fu L 2020 Dmft reveals the non-hermitian topology and fermi arcs in heavy-fermion systems *Phys. Rev. Lett.* **125** 227204
- [17] Matsumoto N, Kawabata K, Ashida Y, Furukawa S and Ueda M 2020 Continuous phase transition without gap closing in non-hermitian quantum many-body systems *Phys. Rev. Lett.* **125** 260601
- [18] Matsumoto N et al 2020 Reciprocal skin effect and its realization in a topoelectrical circuit *Phys. Rev. Res.* **2** 023265
- [19] Chang P-Y, You J-S, Wen X and Ryu S 2020 Entanglement spectrum and entropy in topological non-hermitian systems and nonunitary conformal field theory *Phys. Rev. Res.* **2** 033069
- [20] Vecsei P M, Denner M M, Neupert T and Schindler F 2021 Symmetry indicators for inversion-symmetric non-hermitian topological band structures *Phys. Rev. B* **103** L201114
- [21] Zhang W, Ouyang X, Huang X, Wang X, Zhang H, Yu Y, Chang X, Liu Y, Deng D-L and Duan L-M 2021 Observation of non-hermitian topology with nonunitary dynamics of solid-state spins *Phys. Rev. Lett.* **127** 090501
- [22] Schindler F and Prem A 2021 Dislocation non-hermitian skin effect *Phys. Rev. B* **104** L161106
- [23] Liu H, You J-S, Ryu S and Cosma Fulga I C 2021 Supermetal-insulator transition in a non-hermitian network model *Phys. Rev. B* **104** 155412
- [24] Kawabata K and Ryu S 2021 Nonunitary scaling theory of non-hermitian localization *Phys. Rev. Lett.* **126** 166801
- [25] Sayyad S, Hannukainen J D and Grushin A G 2022 Non-hermitian chiral anomalies *Phys. Rev. Res.* **4** L042004
- [26] Kawabata K, Shiozaki K and Ryu S 2022 Many-body topology of non-hermitian systems *Phys. Rev. B* **105** 165137
- [27] Guo T, Kawabata K, Nakai R and Ryu S 2023 Non-Hermitian boost deformation *Phys. Rev. B* **108** 075108
- [28] Liu H and Cosma Fulga I 2022 Mixed higher-order topology: boundary non-Hermitian skin effect induced by a Floquet bulk *Phys. Rev. B* **108** 035107
- [29] Schindler F, Gu K, Lian B and Kawabata K 2023 Hermitian bulk – non-Hermitian boundary correspondence *PRX Quantum* **4** 030315
- [30] Ju C-Y, Miranowicz A, Chen G-Y and Nori F 2019 Non-hermitian hamiltonians and no-go theorems in quantum information *Phys. Rev. A* **100** 062118
- [31] Gong Z, Bello M, Malz D and Kunst F K 2022 Anomalous behaviors of quantum emitters in non-hermitian baths *Phys. Rev. Lett.* **129** 223601
- [32] Fleckenstein C, Zorzato A, Varjas D, Bergholtz E J, Bardarson J H and Tiwari A 2022 Non-hermitian topology in monitored quantum circuits *Phys. Rev. Res.* **4** L032026
- [33] Kawabata K, Kulkarni A, Li J, Numasawa T and Ryu S 2022 Symmetry of open quantum systems: classification of dissipative quantum chaos (arXiv:2212.00605)
- [34] Xiao Z, Kawabata K, Luo X, Ohtsuki T and Shindou R 2022 Level statistics of real eigenvalues in non-hermitian systems *Phys. Rev. Res.* **4** 043196
- [35] Kawabata K, Numasawa T and Ryu S 2022 Entanglement phase transition induced by the non-Hermitian skin effect *Phys. Rev. X* **13** 021007
- [36] Kawabata K, Shiozaki K and Ueda M 2018 Anomalous helical edge states in a non-hermitian chern insulator *Phys. Rev. B* **98** 165148
- [37] Torres L E F F 2019 Perspective on topological states of non-hermitian lattices *J. Phys. Mater.* **3** 014002
- [38] Edvardsson E, Kunst F K and Bergholtz E J 2019 Non-hermitian extensions of higher-order topological phases and their biorthogonal bulk-boundary correspondence *Phys. Rev. B* **99** 081302
- [39] Kunst F K and Dwivedi V 2019 Non-hermitian systems and topology: a transfer-matrix perspective *Phys. Rev. B* **99** 245116
- [40] Kawabata K, Shiozaki K, Ueda M and Sato M 2019 Symmetry and topology in non-hermitian physics *Phys. Rev. X* **9** 041015
- [41] Liu T, Zhang Y-R, Ai Q, Gong Z, Kawabata K, Ueda M and Nori F 2019 Second-order topological phases in non-hermitian systems *Phys. Rev. Lett.* **122** 076801
- [42] Kawabata K, Higashikawa S, Gong Z, Ashida Y and Ueda M 2019 Topological unification of time-reversal and particle-hole symmetries in non-hermitian physics *Nat. Commun.* **10** 297
- [43] Herviou L, Bardarson J H and Regnault N 2019 Defining a bulk-edge correspondence for non-hermitian hamiltonians via singular-value decomposition *Phys. Rev. A* **99** 052118
- [44] Ashida Y, Gong Z and Ueda M 2020 Non-hermitian physics *Adv. Phys.* **69** 249–435
- [45] Edvardsson E, Kunst F K, Yoshida T and Bergholtz E J 2020 Phase transitions and generalized biorthogonal polarization in non-hermitian systems *Phys. Rev. Res.* **2** 043046
- [46] Kawabata K and Sato M 2020 Real spectra in non-hermitian topological insulators *Phys. Rev. Res.* **2** 033391
- [47] Hamazaki R, Kawabata K, Kura N and Ueda M 2020 Universality classes of non-hermitian random matrices *Phys. Rev. Res.* **2** 023286
- [48] Hua Lee C, Li L, Thomale R and Gong J 2020 Unraveling non-hermitian pumping: emergent spectral singularities and anomalous responses *Phys. Rev. B* **102** 085151
- [49] Kawabata K, Okuma N and Sato M 2020 Non-bloch band theory of non-hermitian hamiltonians in the symplectic class *Phys. Rev. B* **101** 195147
- [50] Bergholtz E J, Carl Budich J C and Kunst F K 2021 Exceptional topology of non-hermitian systems *Rev. Mod. Phys.* **93** 015005
- [51] Koch R and Carl Budich J C 2020 Bulk-boundary correspondence in non-hermitian systems: stability analysis for generalized boundary conditions *Eur. Phys. J. D* **74** 70
- [52] Xiao L, Deng T, Wang K, Zhu G, Wang Z, Yi W and Xue P 2020 Non-hermitian bulk–boundary correspondence in quantum dynamics *Nat. Phys.* **16** 761–6
- [53] Michael Denner M, Skurativska A, Schindler F, Fischer M H, Thomale R, Bzdušek T and Neupert T 2021 Exceptional topological insulators *Nat. Commun.* **12** 5681
- [54] Kawabata K, Shiozaki K and Ryu S 2021 Topological field theory of non-hermitian systems *Phys. Rev. Lett.* **126** 216405
- [55] Stegmaier A et al 2021 Topological defect engineering and \mathcal{PT} symmetry in non-hermitian electrical circuits *Phys. Rev. Lett.* **126** 215302
- [56] Vyas V M and Roy D 2021 Topological aspects of periodically driven non-hermitian su-schrieffer-heeger model *Phys. Rev. B* **103** 075441
- [57] Zhou H and Yeon Lee J Y 2019 Periodic table for topological bands with non-hermitian symmetries *Phys. Rev. B* **99** 235112
- [58] Yeon Lee J Y, Ahn J, Zhou H and Vishwanath A 2019 Topological correspondence between hermitian and non-hermitian systems: anomalous dynamics *Phys. Rev. Lett.* **123** 206404
- [59] Kawabata K, Sato M and Shiozaki K 2020 Higher-order non-hermitian skin effect *Phys. Rev. B* **102** 205118
- [60] Xiong Y 2018 Why does bulk boundary correspondence fail in some non-hermitian topological models *J. Phys. Commun.* **2** 035043

- [61] Yao S and Wang Z 2018 Edge states and topological invariants of non-hermitian systems *Phys. Rev. Lett.* **121** 086803
- [62] Kunst F K, Edvardsson E, Carl Budich J C and Bergholtz E J 2018 Biorthogonal bulk-boundary correspondence in non-hermitian systems *Phys. Rev. Lett.* **121** 026808
- [63] Martinez Alvarez V M, Barrios Vargas J E and Foa Torres L E F 2018 Non-hermitian robust edge states in one dimension: Anomalous localization and eigenspace condensation at exceptional points *Phys. Rev. B* **97** 121401
- [64] Hua Lee C H and Thomale R 2019 Anatomy of skin modes and topology in non-hermitian systems *Phys. Rev. B* **99** 201103
- [65] Helbig T, Hofmann T, Imhof S, Abdelghany M, Kiessling T, Molenkamp L W, Lee C H, Szameit A, Greiter M and Thomale R 2020 Generalized bulk-boundary correspondence in non-hermitian topoelectrical circuits *Nat. Phys.* **16** 747–50
- [66] Okuma N, Kawabata K, Shiozaki K and Sato M 2020 Topological origin of non-hermitian skin effects *Phys. Rev. Lett.* **124** 086801
- [67] Weidemann S, Kremer M, Helbig T, Hofmann T, Stegmaier A, Greiter M, Thomale R and Szameit A 2020 Topological funneling of light *Science* **368** 311–4
- [68] Borgnia D S, Jura Kruchkov A and Slager R-J 2020 Non-hermitian boundary modes and topology *Phys. Rev. Lett.* **124** 056802
- [69] Okuma N and Sato M 2020 Hermitian zero modes protected by nonnormality: application of pseudospectra *Phys. Rev. B* **102** 014203
- [70] Gong Z, Ashida Y, Kawabata K, Takasan K, Higashikawa S and Ueda M 2018 Topological phases of non-hermitian systems *Phys. Rev. X* **8** 031079
- [71] Michael Denner M and Schindler F 2022 Magnetic flux response of non-hermitian topological phases *SciPost Phys.* **14** 107
- [72] Nakamura D, Bessho T and Sato M 2022 Bulk-boundary correspondence in point-gap topological phases (arXiv:2205.15635)
- [73] Kawabata K, Bessho T and Sato M 2019 Classification of exceptional points and non-hermitian topological semimetals *Phys. Rev. Lett.* **123** 066405
- [74] Sayyad S and Kunst F K 2022 Realizing exceptional points of any order in the presence of symmetry *Phys. Rev. Res.* **4** 023130
- [75] Sayyad S, Stalhammar M, Rodland L and Kunst F K 2022 Symmetry-protected exceptional and nodal points in non-Hermitian systems (arXiv:2204.13945)
- [76] Mudry C, Simons B D and Altland A 1998 Random dirac fermions and non-hermitian quantum mechanics *Phys. Rev. Lett.* **80** 4257–60
- [77] Mudry C, Brouwer P W, Halperin B I, Gurarie V and Zee A 1998 Density of states in the non-hermitian lloyd model *Phys. Rev. B* **58** 13539–43
- [78] Ryu S, Schnyder A P, Furusaki A and Ludwig A W W 2010 Topological insulators and superconductors: tenfold way and dimensional hierarchy *New J. Phys.* **12** 065010
- [79] The supplemental material contains exhaustive auxiliary derivations and toy model Hamiltonians realising intrinsic point gap topology
- [80] Schindler F 2020 Dirac equation perspective on higher-order topological insulators *J. Appl. Phys.* **128** 221102
- [81] Shen H, Zhen B and Fu L 2018 Topological band theory for non-hermitian hamiltonians *Phys. Rev. Lett.* **120** 146402
- [82] Yang Z, Schnyder A P, Hu J and Chiu C-K 2021 Fermion doubling theorems in two-dimensional non-hermitian systems for fermi points and exceptional points *Phys. Rev. Lett.* **126** 086401
- [83] Lukas J, König K, Yang K, Budich J C and Bergholtz E J 2022 Braid protected topological band structures with unpaired exceptional points (arXiv:2211.05788)
- [84] Alsallom F, Herviou L, Yazyev O V and Brzezińska M 2022 Fate of the non-hermitian skin effect in many-body fermionic systems *Phys. Rev. Res.* **4** 033122
- [85] Komis I, Kaltsas D, Xia S, Buljan H, Chen Z and Makris K G 2022 Robustness versus sensitivity in non-hermitian topological lattices probed by pseudospectra *Phys. Rev. Res.* **4** 043219